Supporting Information

In situ unraveling effect of dynamic chemical state on selective CO_2 reduction upon zinc electrocatalyst

Tai-Lung Chen,‡[a] Hsiao-Chien Chen,‡[a,b] Yen-Po Huang,[a] Sheng-Chih Lin,[a] Cheng-Hung Hou,[c] Hui-Ying Tan,[a] Ching-Wei Tung,[a] Ting-Shan Chan,*[d] Jing-Jong Shyue,[c,e] and Hao Ming Chen*[a,d]

[a]*Department of Chemistry, National Taiwan University, Taipei 10617, Taiwan, E-mail: haomingchen@ntu.edu.tw*
[b]*Department of Photonics, National Cheng Kung University, Tainan 70101, Taiwan*
[c]*Research Center for Applied Sciences, Academia Sinica, Taipei 11529, Taiwan*
[d]*National Synchrotron Radiation Center, Hsinchu 30076, Taiwan*
[e]*Department of Materials Science and Engineering, National Taiwan University, Taipei 10617, Taiwan*

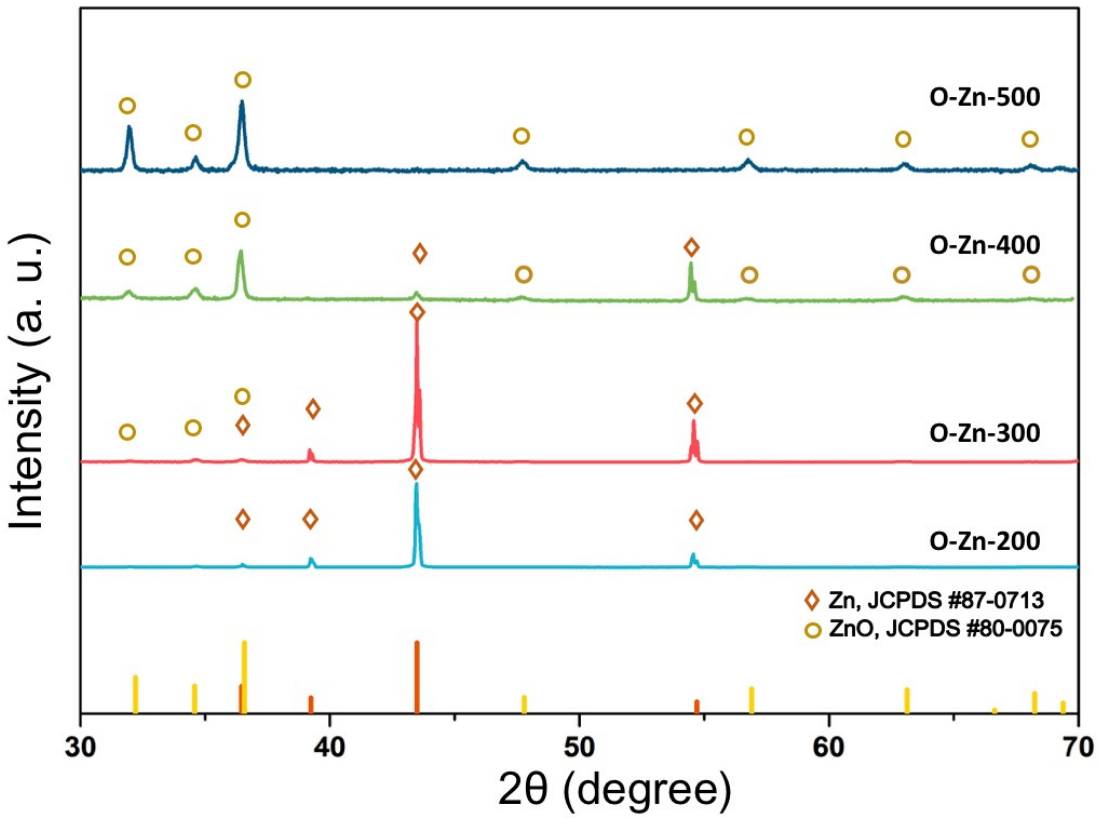

Fig. S1 X-ray diffraction patterns of O-Zn-200, O-Zn-300, O-Zn-400 and O-Zn-500.

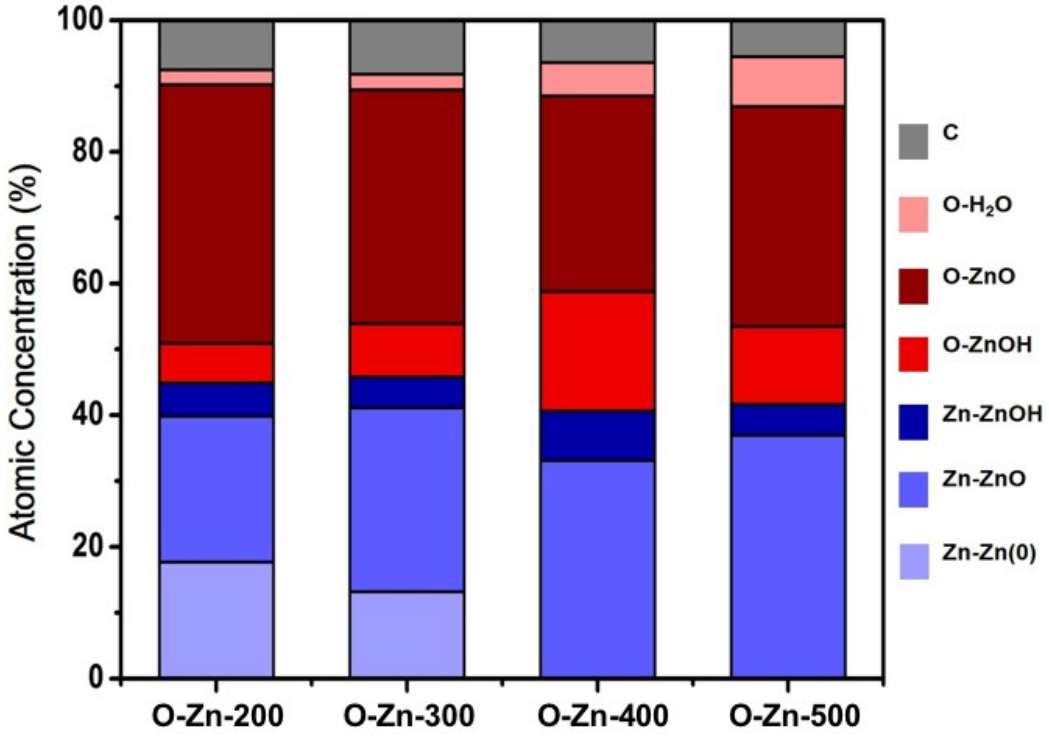

Fig. S2 XPS quantitation analysis atomic ratio of all species contained in O-Zn-200, O-Zn-300, O-Zn-400 and O-Zn-500.

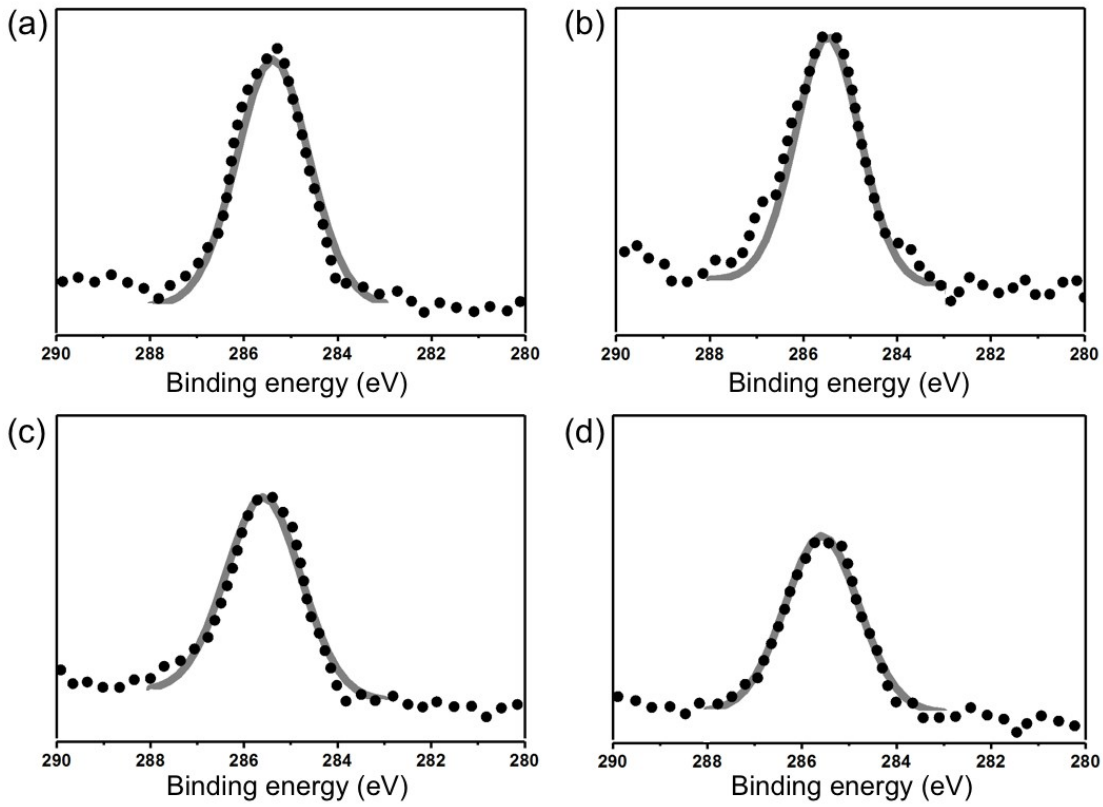

Fig. S3 XPS spectra of C 1s of (a) O-Zn-200, (b) O-Zn-300, (c) O-Zn-400 and (d) O-Zn-500.

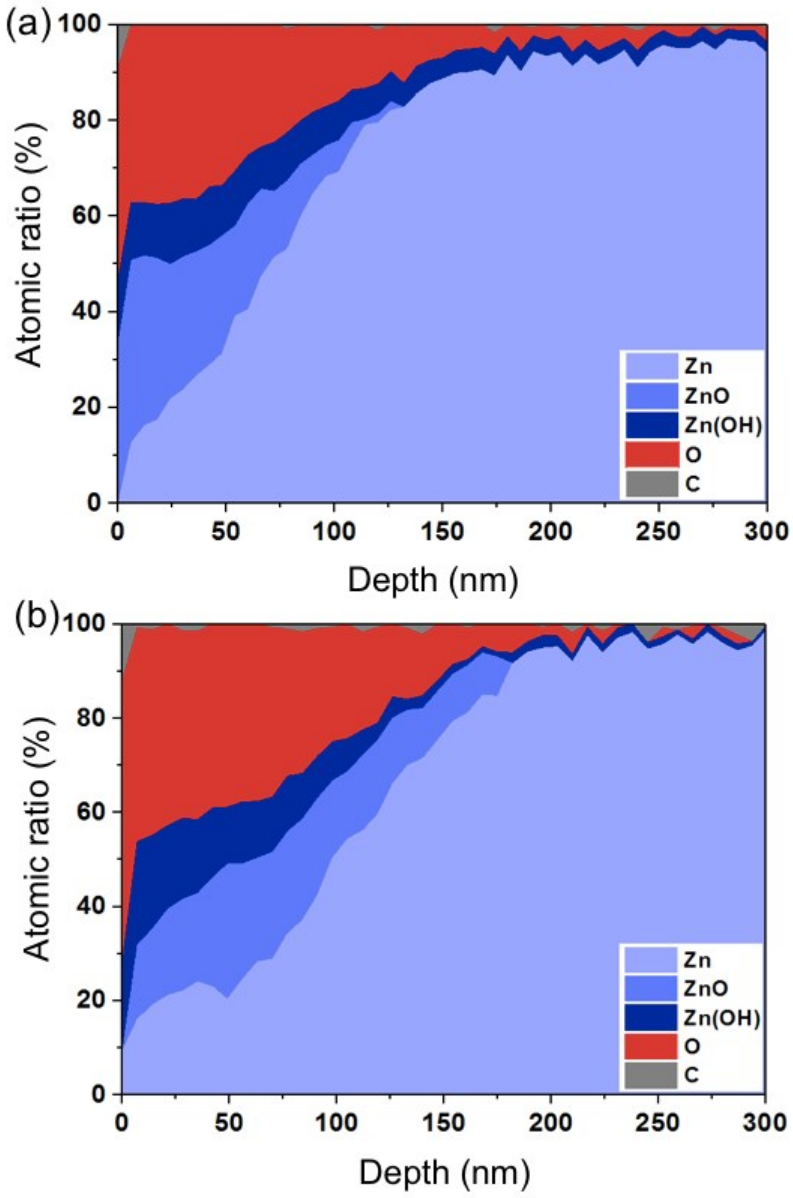

Fig. S4 Depth-profiling XPS of (a) O-Zn-200 and (b) O-Zn-400.

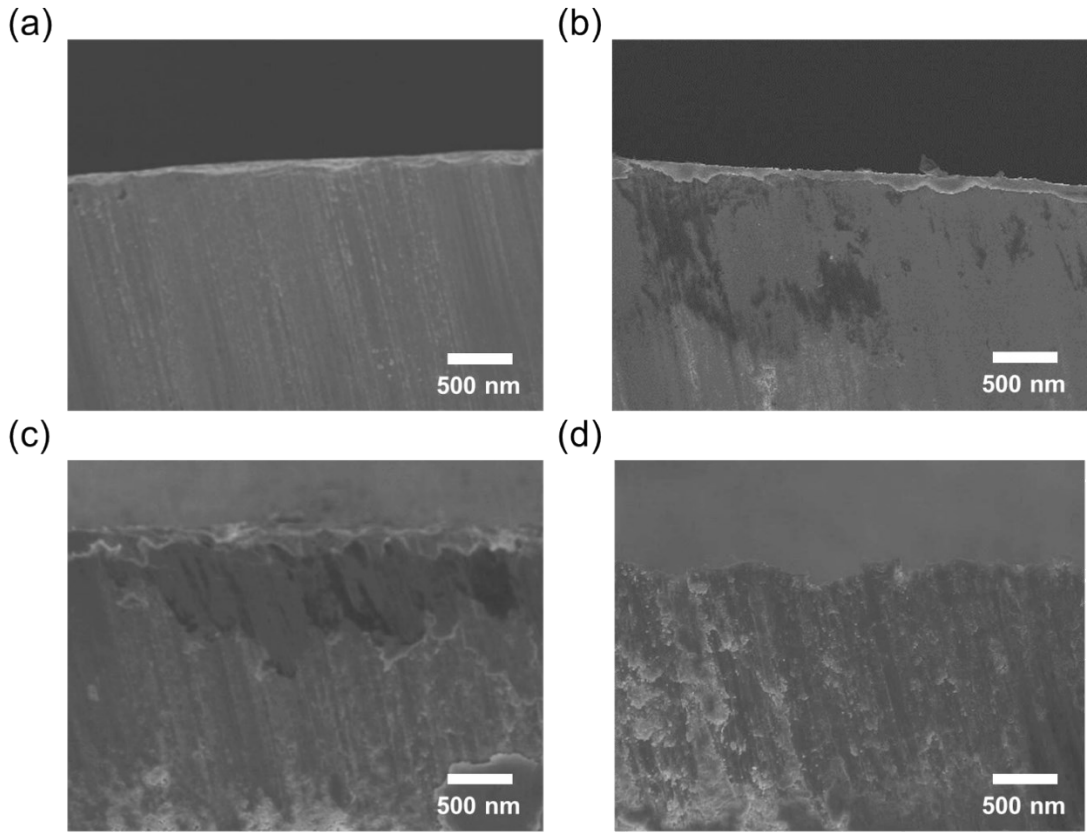

Fig. S5 Cross-section SEM images of (a) O-Zn-200, (b) O-Zn-300, (c) O-Zn-400 and (d) O-Zn-500.

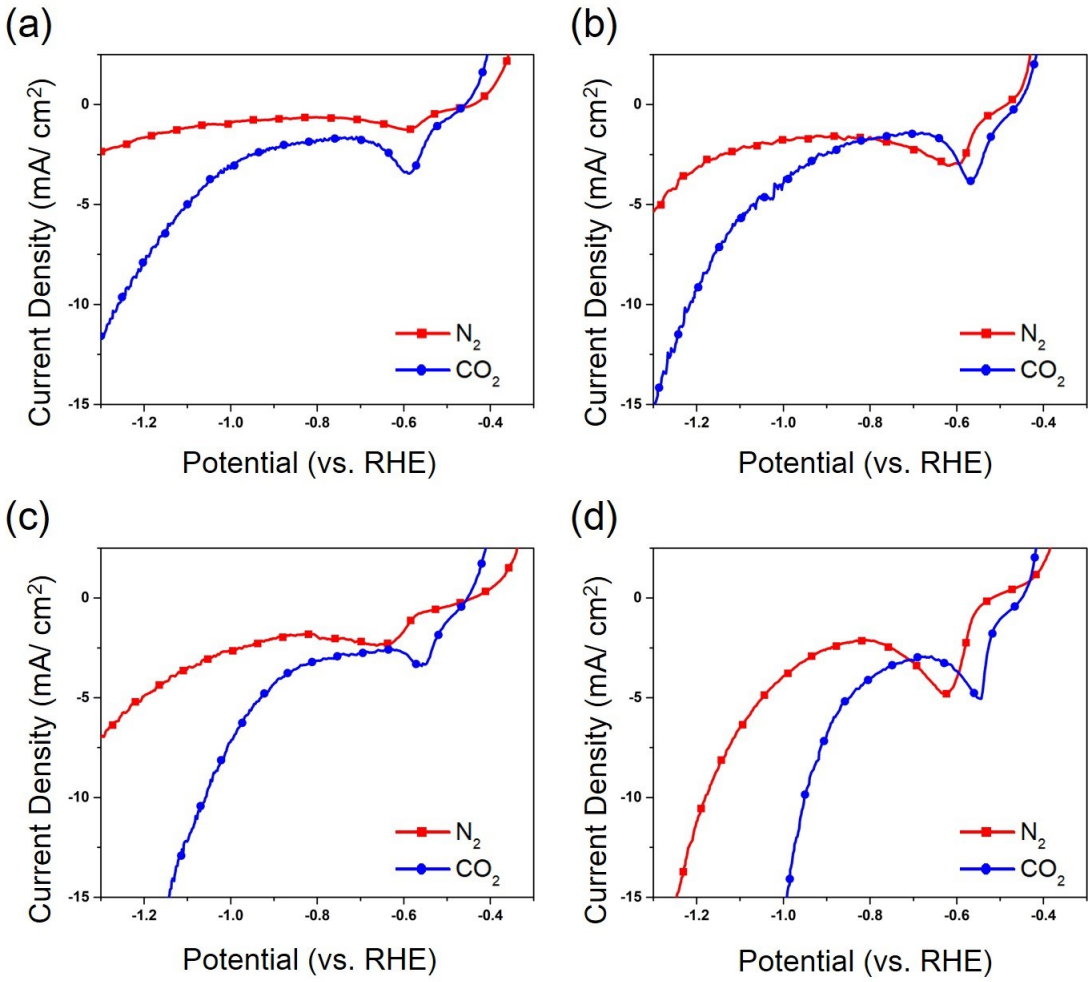

Fig. S6 CO_2RR performance analysis. LSV measurements under in 0.1M $KHCO_3$ with saturated CO_2 or N_2 of (a) O-Zn-200, (b) O-Zn-300, (c) O-Zn-400 and (d) O-Zn-500.

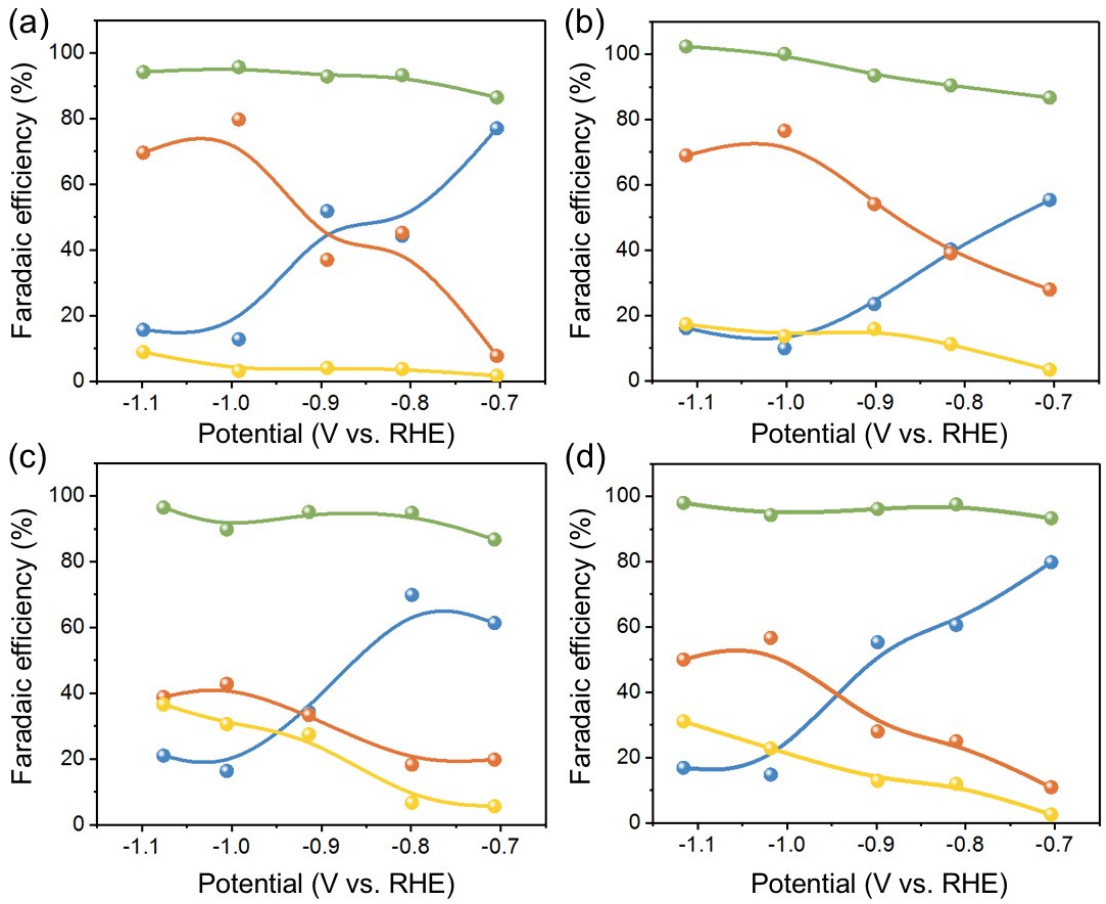

Fig. S7 Faradaic efficiency performance at a selected potential window between − 0.70 to −1.10 V (vs. RHE) of (a) O-Zn-200, (b) O-Zn-300, (c) O-Zn-400 and (d) O-Zn-500. Faradaic efficiency of CO (orange), formate (yellow), H_2 (blue) and total faradaic efficiency (green) of each samples were shown in the figure.

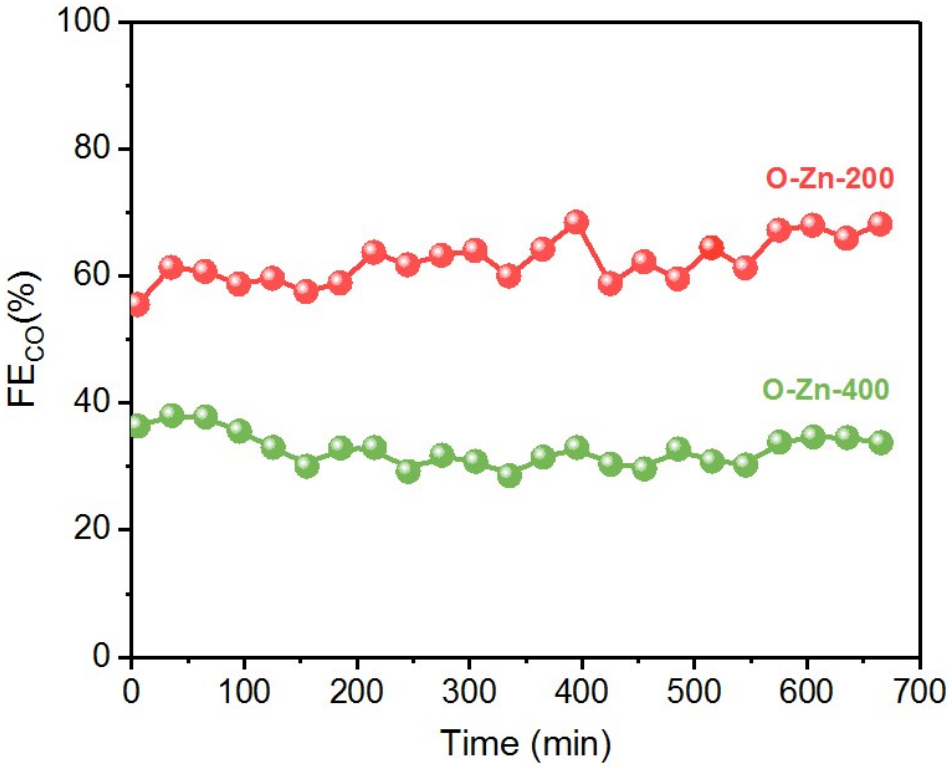

Fig. S8 The stability of O-Zn-200 and O-Zn-400 at cathodic potential of -1.0 V during CO_2RR.